ACS APPLIED MATERIALS & INTERFACES

www.acsami.org

Research Article

Waterproof, Highly Tough, and Fast Self-Healing Polyurethane for Durable Electronic Skin

Wu Bin Ying,[#] Zhe Yu,[#] Do Hwan Kim, Kyung Jin Lee, Han Hu, Yiwei Liu, Zhengyang Kong, Kai Wang, Jie Shang,* Ruoyu Zhang,* Jin Zhu, and Run-Wei Li

Cite This: *ACS Appl. Mater. Interfaces* 2020, 12, 11072−11083

Read Online

ACCESS | Metrics & More | Article Recommendations | Supporting Information

ABSTRACT: A stretchable electronic skin (e-skin) requires a durable elastomeric matrix to serve in various conditions. Therefore, excellent and balanced properties such as elasticity, water proof capability, toughness, and self-healing are demanded. However, it is very difficult and often contradictory to optimize them at one time. Here, a polyurethane (BS-PU-3) containing a polydisperse hard segment, hydrophobic soft segment, and a dynamic disulfide bond was prepared by one-pot synthesis. Unlike the normal two-pot reaction, BS-PU-3 obtained through the one-pot method owned a higher density of self-healing points along the main chain and a faster self-healing speed, which reached 1.11 μm/min in a cut-through sample and recovered more than 93% of virgin mechanical properties in 6 h at room temperature. Moreover, a remarkable toughness of 27.5 MJ/m^3 assures its durability as an e-skin matrix. Even with a 1 mm notch (half of the total width) on a standard dumbbell specimen, it could still bear the tensile strain up to 324% without any crack propagation. With polybutadiene as the soft segment, the shape, microstructure, and conductivity in BS-PU-3 and BS-PU-3-based stretchable electronics kept very stable after soaking in water for 3 days, proving the super waterproof property. An e-skin demo was constructed, and self-healing in pressure sensitivity, mechanical, and electrical properties were verified.

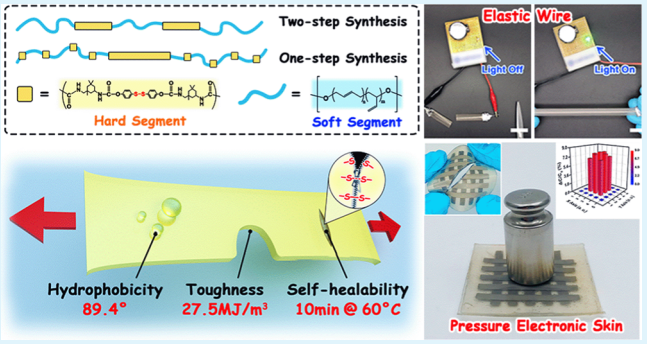

KEYWORDS: *polyurethane, toughness, water proof, self-healing, electronic skin*

1. INTRODUCTION

Stretchable electronic skin (E-skin) is a kind of flexible and wearable electronic device that simulates the mechanical properties and tactile perception of real human skin, which can be used in a wide range of applications such as human−computer interaction, intelligent prosthetics, medical rehabilitation, and so forth.[1−3] As an electronic device, the stretchable e-skin is assembled from several functional units, mainly including circuits, electrodes, sensing units, and the like.[4,5] These units are usually based on a polymer elastomer matrix and filled with a multifunctional conductive filler to achieve various functions. An ideal e-skin should be close to human skin in all aspects, such as stretching and resilience, water stability, self-healing, and so forth. As one of the core materials, the polymer elastic matrix not only determines the mechanical properties of the stretchable E-skin but also needs to realize multifunctions.[6]

Polyurethane (PU) has a soft segment with a lower glass-transition temperature (T_g) and a hard segment with a higher T_g.[7,8] In the condensed state, these two thermodynamically incompatible components undergo microphase separation, forming a soft matrix and hard domains, respectively. With low T_g, the soft matrix endows the material with deformability, whereas the hard domains having a strong hydrogen-bond interaction or in a crystalline state provide good shape fixity. Because of the inhomogeneity in the microstructure, PU exhibits good toughness and tear resistance compared to other homopolymer elastomers.[9] At the same time, the desired modulus and deformation ability of the elastic matrix can be obtained by adjusting the ratio between the soft and hard segments. In addition, PU has the advantages of feasible molecular design and functionalization.[10−12] Vast amounts of macromolecular diols can be used as soft segments, whereas lots of diisocyanates and chain extenders are the candidates of the hard segment. The functionalization of the soft segment and hard segment could be realized by simply introducing various functional groups into the macromolecular diols, diisocyanates, and chain extenders. Because of the remarkable and flexible mechanical properties, PU-based functional matrixes are getting more and more attention.[7,13−15]

Received: January 10, 2020
Accepted: February 11, 2020
Published: February 11, 2020

https://dx.doi.org/10.1021/acsami.0c00443
ACS Appl. Mater. Interfaces 2020, 12, 11072−11083

The advancement in e-skin area is fast. Well-performed mechanical properties are not enough for this area now, and properties like self-healing, waterproof, and good toughness are demanded.[5,6,16−18] As a wonderful candidate for elastic matrix in the stretchable E-skin, PU is capable of realizing the above functions. In the study of self-healing PUs, scientists have often introduced reversible (dynamic) covalent bonds or self-assembly groups to achieve goals, such as hydrogen bonds,[19,20] Diels−Alder reactions,[21] metal−ligand interactions,[22] urea chemistry,[23,24] disulfide metathesis, and so on.[25−27] However, PU has a strong hydrophilicity because of the presence of urethane bonds in the hard segments and usually contains polyether−polytetrahydrofuran as the soft segment, making it easy to absorb water in a humid environment, which may cause signal interference for e-skin.[28−32] Therefore, the development of self-healing and intrinsic hydrophobicity for PU is an important prerequisite for ensuring the stable operation of the e-skin device.

Herein, the current investigation designed the structures of both the soft segment and hard segment to render PU elasticity, toughness, self-healing capability, and waterproof property. Specifically, the hydroxyl-terminated polybutadiene (HTPB) was selected as the soft segment to enhance the hydrophobicity for the resulting PU. Bis(4-hydroxyphenyl)-disulfide (HPS) was used as the chain extender, which could offer the dynamic disulfide bond for the self-healing function. The microphase-separated structure provided elasticity and dramatically increased the toughness of the PU when compared with the structure of homogeneous polymers such as polydimethylsiloxane (PDMS). Based on the above strategy, we synthesized and selected a PU exhibiting good elasticity, excellent toughness, fast self-healing speed at room temperature, and super waterproof property. Finally, with this multifunctional PU used as the elastic matrix and liquid metal gallium−indium−tin alloy (galinstan, GaInSn) as the conductive filler, we were able to prepare a demo e-skin.

2. EXPERIMENTAL SECTION

2.1. Materials. HTPB (M_n = 3000 g mol^{-1}) was purchased from Tianyuan Institute of Chemical Research, and the OH index was exactly titrated before use. Isophorone diisocyanate (IPDI, 99%), dibutyltin dilaurate (DBTDL, 95%), anhydrous tetrahydrofuran (THF, 99.5%), tetrachloroethane (TCE, 99.5%), and HPS (98%) were purchased from Aladdin (China) without further purification. Gallium (99.99%), indium (99.995%), and tin (99.99%) were all purchased from Beijing Founde Star Sci. & Technol. Co., Ltd. Commercial PU 1180A was purchased from BASF Co., Ltd. with a hardness of 80 Shore A, which is a commonly used PU.

2.2. PU Synthesis. *2.2.1. One-Pot Synthesis.* A typical polymerization procedure for BS-PU (BS-PU-1) is described below. In the glovebox filled with 99.999% Ar, fresh HTPB (10 g) was poured into a dried three-neck reactor equipped with a mechanical stirrer, followed by the addition of IPDI (5.44 g), DBTDL (0.2 g), HPS (5 g), and THF (50 mL). The stoichiometric ratio of [NCO]/[OH] was kept and the final concentration was adjusted to 30 wt % in this system. Then, the whole system was heated at 65 °C for 8 h to obtain the complete polymerization. In the end, the polymer was precipitated into excess distilled water and washed several times, followed by drying in a vacuum at 60 °C for 24 h to constant weight. The wt % ratios of [HTPB]/[HPS] were varied by 2/1 (BS-PU-1), 3/1 (BS-PU-2), 4/1 (BS-PU-3), and 5/1 (BS-PU-4) for various PUs with different disulfide contents and hard segments.

2.2.2. Two-Pot Synthesis. In the glovebox filled with 99.999% Ar, fresh HTPB (12 g) was poured into a dried three-neck reactor equipped with a mechanical stirrer, followed by the addition of IPDI (3.56 g), DBTDL (0.2 g), and THF (15 mL). Then, the reactor was sealed by a rubber septum and moved to a 65 °C oil bath for 1 h before polymerization. After this, a designed amount of HPS (3 g) was dissolved in THF, and the resulting solution was injected dropwise into the sealed reactor for PU chain extension. The stoichiometric ratio of [NCO]/[OH] was kept and the final concentration was adjusted to 30 wt % in this system. Then, the whole system was heated at 65 °C for another 6 h to obtain the complete polymerization. In the end, the polymer was precipitated into excess distilled water and washed several times, followed by drying in a vacuum at 60 °C for 24 h to constant weight.

2.3. Film Preparation. A 30 wt % PU solution in TCE was loaded into a square Teflon mold with the dimensions of 70 mm × 70 mm × 10 mm. The mold was gradually dried under hood over 24 h, followed by heating at 60 °C for another 24 h. The residual solvent was removed by vacuum drying at 60 °C for 12 h. A thin PU film (thickness ≈ 0.4 mm) without any bubble could be obtained in this way.

2.4. Preparation of Flexible Electronic Devices Based on Synthetic PUs. *2.4.1. Elastic Conductive Wire.* First, gallium, indium, and tin were mixed and stirred at 60 °C for 0.5 h in the ratio of 68.2:21.8:10 by mass to obtain galinstan. Second, galinstan was mixed with the concentrated PU solution in the ratio of galinstan/PU = 16:1 (wt/wt) to obtain a mushy conductive ink used as a composite conductor (liquid metals@PU). Then, the mushy conductive ink was printed on the PU thin film by a homemade direct ink writing equipment. Further, the PU film with the printed ink was heated to 80 °C for 24 h for drying. Finally, the elastic and conductive wire was obtained by pouring the PU solution onto the film and coating onto the composite conductor.

2.4.2. Capacitive Pressure-Sensing E-Skin. First, a stencil with a desired carved pattern was stuck to the PU thin film. Second, the aforementioned mushy conductive ink was loaded on the stencil and squeegeed through the stencil. Then, the stencil was removed to leave the mushy conductive ink with the desired pattern, followed by drying at 80 °C for 24 h. Further, the concentrated PU solution was poured onto the film and dried to get the electrode layer of pressure-sensing e-skin. Lastly, the capacitive pressure-sensing e-skin was obtained by sticking two electrode layers orthogonally.

2.5. Characterizations. The self-healing test was carried out as follows: the 0.4 mm PU film was cut to several small rectangular films, and the middle portion of the small rectangular film was completely cut off for the self-healing test. The scratch recovery was observed under an optical microscope (Olympus/BX 51TF Instec H601, Japan) equipped with a hot stage at various temperatures and for various time periods. Small-angle X-ray scattering (SAXS) experiments were carried out on a Xeuss SAXS system of Xenocs in Ningbo University with a 0.154 nm X-ray wavelength, and the obtained data were analyzed by the Fit2D software quantitatively. The ^{1}H nuclear magnetic resonance (NMR) spectra were measured on AVANCE III (400 MHz) at room temperature with tetramethylsilane as an internal standard, and the sample concentrations were in the range of 1−5 wt %. The molecular weights and molecular weight distributions of the PUs were analyzed by gel permeation chromatography (GPC), using a GPC column (Waters-2690) at 40 °C, equipped with a refractive index detector using THF as the eluent. The attenuated total reflectance−Fourier transform infrared (ATR−FTIR) absorption spectra were measured on an iD5 ZnSe ATR instrument (Cary660, Agilent). Dynamic mechanical thermal analysis was performed using a DMA Q800 system from TA Instruments (USA). The measurements were carried out at a heating and cooling rate of 3 °C min^{-1} from −120 to 100 °C in a liquid N_2 atmosphere with a frequency of 1 Hz. The mechanical properties of the samples were measured with a universal testing machine (UTM, Instron Instruments, model: 5567), and the extension rate was kept at 5 mm·min^{-1}. Water contact angle analysis was performed on a contact angle goniometer (OCA25, DataPhysics, Germany). The water droplet was deposited using a syringe pointed downward toward the sample film surface. The electronic properties of the prepared stretchable electronic devices based on PU were measured by a dc current source (Keithley 6221), a

https://dx.doi.org/10.1021/acsami.0c00443
ACS Appl. Mater. Interfaces 2020, 12, 11072−11083

nanovoltmeter (Agilent 34420A), and an inductance−capacitance−resistance meter (IM 3570, HIOKI Impedance Analyzer).

3. RESULTS AND DISCUSSION

Copper et al. once studied the difference of segmental distribution in PUs prepared by the one-pot and two-pot synthesis methods.[33−36] Briefly, the two-pot method was the reaction in which polydiol and diisocyanate reacted first, followed by the chain extension by the addition of diols. With this method, the resultant PU usually had a relatively uniform length distribution of the hard segment[33,34] (Scheme 1a, first line). The one-pot method was the reaction in which the mixture of polydiol and diol reacted with diisocyanate in one step. As the diol was a small molecule, its reactivity with diisocyanate was much higher than that of polydiol. As a result, a very long-length hard segment formed in the one-pot sample.[33,35,36] Nevertheless, the mole amount of diisocyanate was excessive, and many short hard segments with diisocyanate as the two ends would directly react with polydiol and formed short hard segments, which widely dispersed between the soft segments (Scheme 1a, second line). Every hard segment containing dynamic disulfide bonds could act as one self-healing point. The number density of the hard segment along the main chain affects the self-healing efficiency. It is also well-known that because of the thermodynamic incompatibility, the soft and hard segments could microphase-separate into a soft phase and a hard domain, respectively.[37,38] The hard domain was connected with the soft phase, and a physical cross-linking network is constructed with the rubbery soft phase anchored among the hard domains.[39−42] In such morphology, the hard domain associated by the hydrogen-bonded hard segment constitutes the node, and the soft phase based on polybutadiene constitutes the deformable matrix (Scheme 1b). As the node of the network structure, the hard domain played an important role in increasing the toughness and tear resistance for the PU materials.[39,42] At the notched region, the tearing process would be retarded or even stopped by the strong nodes because of their fixing capability on the whole network structure and dissipation of the elastic energy. In this way, the notch did not expand during the stretching process, and it gradually developed into an arch shape (Scheme 1c). After the strain was released, the widely dispersed dynamic disulfide bonds could quickly repair the notch through the process of disulfide metathesis, which greatly enhanced the durability of the PU product. In addition, polybutadiene was used as the soft segment to enhance the hydrophobicity of PU.[43,44] As the hydrophilic urethane bonds were embedded in the polybutadiene matrix, the overall hydrophobicity of the PU material was maintained.

Scheme 1. Molecular Design of PU (a) Chemical Structure of BS-PUs; (b) Ideal Network Structure Composed from Soft Phase and Hard Phase; (c) Schematic of an Elongated PU Film with Water Droplets Unable to Infiltrate (Left), Enlarged Notch in Arch Shape with No Crack Propagation (Middle), and the Crack Could be Self-Healed Driven by Dynamic Disulfide Bonds (Right)

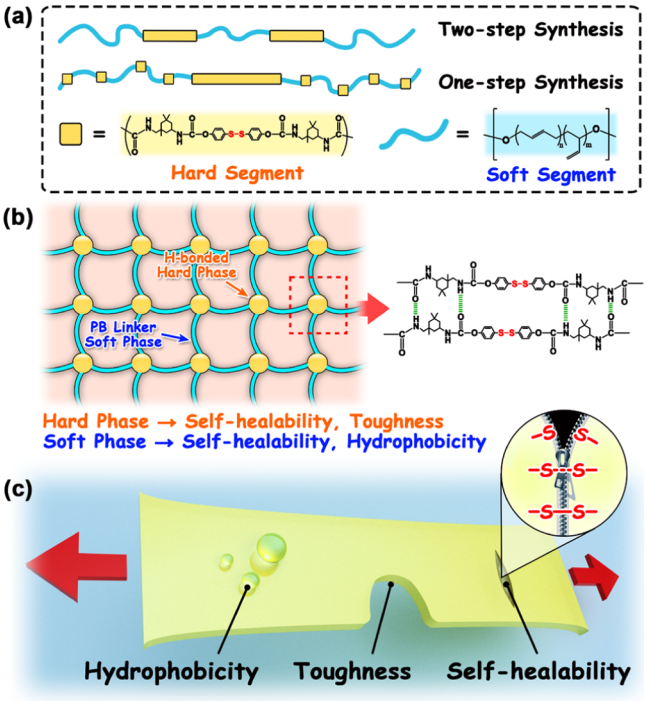

In this work, we intentionally used one-pot polycondensation reaction to prepare the PUs (Supporting Information, Figure S1), that is, HTPB, HPS, and IPDI were simultaneously added in the reactor. In this case, polybutadiene was used as the component of the soft segment, whereas HPS and IPDI together acted as the hard segment. Because of the large steric effect of HTPB, the reaction probability between HPS and IPDI was much higher than that of HTPB. As a result, long-length hard segments formed quickly. As analyzed in the above paragraph, short-length hard segments formed later and would react with HTPB when the two molecules were close enough. As a result, one part of the hard segments was long, whereas the other part was short and widely dispersed between the soft segments (Scheme 1a, second line) and largely improved the self-healing speed.

Four kinds of PUs (BS-PU-#) with different ratios of soft and hard segments were synthesized by the one-pot method, and the structural information and compositions are shown in Figure S2 and summarized in Table S1 (Supporting Information). We analyzed the segmental sequence by using ^{13}C NMR spectroscopy (Supporting Information, Figure S3A). As BS-PU-3 owned the best overall property as will be shown later, we took BS-PU-3 as an example. Its peak at 151.5 ppm represented the terminal carbon of IPDI in the hard segment connected with another hard segment, whereas the peak at 153 ppm represented the one connected to the soft segment of HTPB. Therefore, it could be calculated from the ratio of the two peak areas that about 57.8% of the hard segment was next to the soft segment. In order to compare the dependence of the self-healing efficiency on the disulfide bond distribution, BS-PU-3-2pot with the same recipe as that of BS-PU-3 was synthesized by the two-pot method (Supporting Information, Figure S4). It turned out that only 48.9% of the hard segment was next to the soft segment in this two-pot sample, which was lower than that of the one-pot-synthesized BS-PU-3 (Supporting Information, Figure S3B). The illustration of the hard segment about their length and distribution in Scheme 1a was verified. More hard segments adjacent to the soft segments meant higher density of self-healing points.

The four synthesized BS-PU-1−4 exhibited very competitive mechanical properties when compared to many other counterparts[45−50] (Figure 1a, Supporting Information Table S2). By adjusting the molar ratio of the hard and soft segments, we

https://dx.doi.org/10.1021/acsami.0c00443
ACS Appl. Mater. Interfaces 2020, 12, 11072−11083

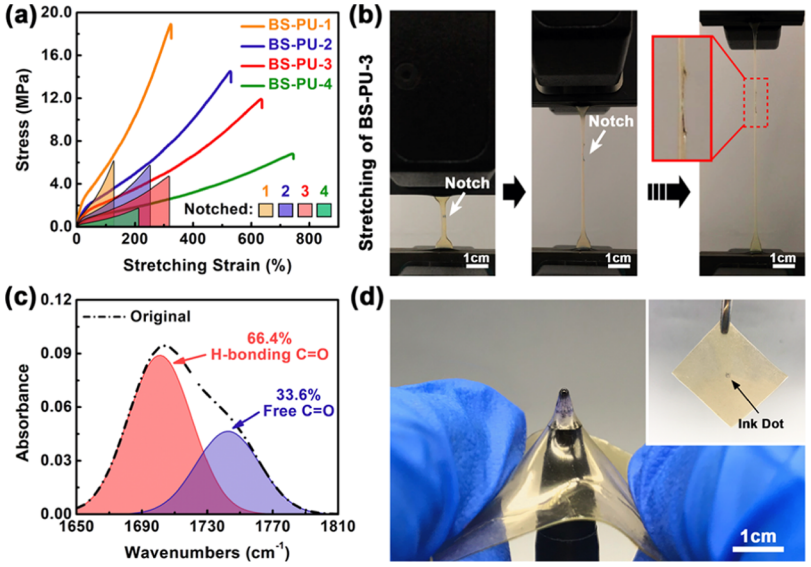

Figure 1. (a) Typical strain−stress curves of original and notched BS-PU samples. Sample: standard dumbbell specimen (ASTM D412) having a 0.4 mm thickness; (b) a notched BS-PU-3 specimen before stretch (left) and at a strain of 324% (right) in a UTM showing that this material can prevent crack propagation; (c) FTIR absorbance spectra in the C═O stretching region of BS-PU-3 (black dotted line): the band at 1700 cm^{-1} (red filled area) and 1745 cm^{-1} (blue filled area) represented H-bonded and free C═O stretching, respectively; (d) puncture demonstration of BS-PU-3 with a pen, and the illustration was the film after puncture (top right).

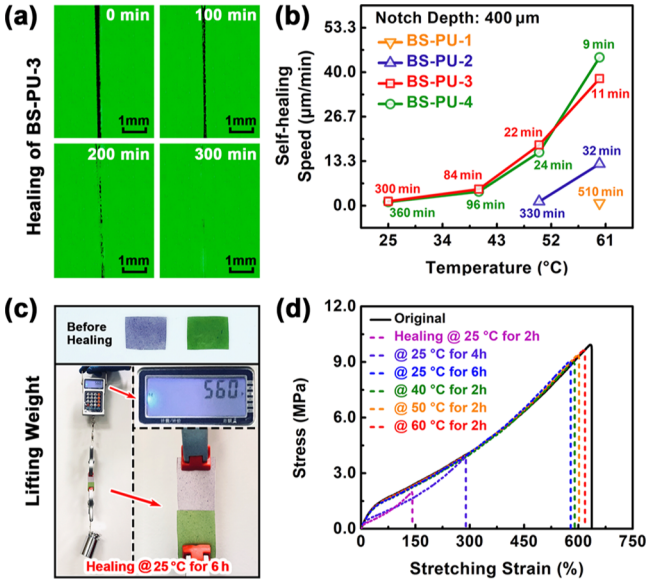

Figure 2. (a) Optical microscope images of the notched and self-healed BS-PU-3 film showing a gradual disappearance of the scar during self-healing at room temperature for 300 min; (b) self-healing speed for notched BS-PU samples at different temperatures calculated from [notch size]/[self-healing period], and the completion time of self-healing was marked beside the curves; (c) images of the dyed BS-PU-3 film with ∼1 mm thickness that was cut into two pieces, followed by self-healing at room temperature, and subjected to a 560 g weightlifting test; (d) stress−strain curves of the notched BS-PU-3 self-healing at 25 °C for different times and at 40−60 °C for 2 h, showing a better recoverability of mechanical properties when self-healed for a longer time or at a higher temperature.

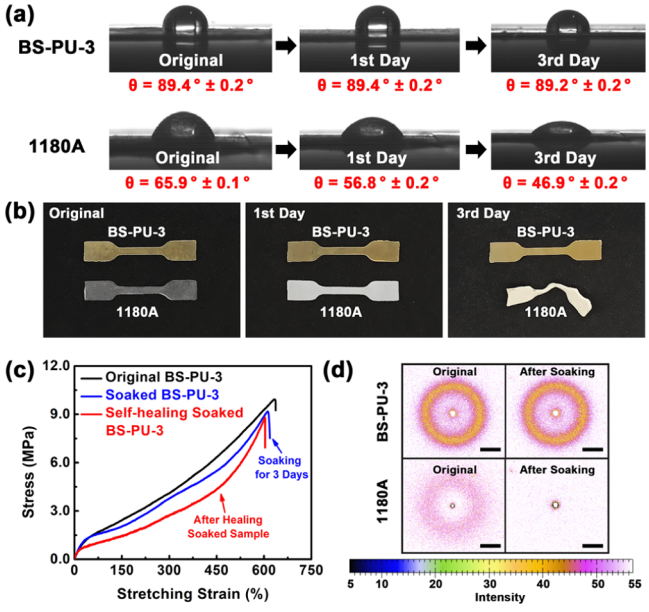

Figure 3. (a) Images of the water contact angles of BS-PU-3 and 1180A after being soaked in water for 0, 1, and 3 days, representing the changes in their hydrophobicity; (b) images of standard specimens BS-PU-3 and 1180A after being soaked in water for 0, 1, and 3 days, representing the shape deformation; (c) stress−strain curves of original BS-PU-3, BS-PU-3 soaked in water for 3 days, and the soaked BS-PU-3 after self-healing, showing its excellent hydrophobicity and unaffected self-healing capability after water absorption; (d) 2D-SAXS patterns of original BS-PU-3, original 1180A, and samples after 3 days of soaking, representing changes in the microstructure after longtime water absorption. The scale bar was 0.3 nm^{-1}.

could tune the overall mechanical properties of the PU materials. As the soft segment content increased from BS-PU-1 to BS-PU-4, the deformability was gradually improved, but the tensile modulus decreased. The easy-to-regulate performances of PU provided attractive advantages for the selection of the e-skin matrix. Moreover, all BS-PUs showed remarkable toughness (15.9−27.5 MJ/m^3), as summarized in Table S2. For BS-PU-3 with toughness up to 27.5 MJ/m^3, its tear resistance property was tested, as shown in Figure 1a (filled

https://dx.doi.org/10.1021/acsami.0c00443
ACS Appl. Mater. Interfaces 2020, 12, 11072−11083

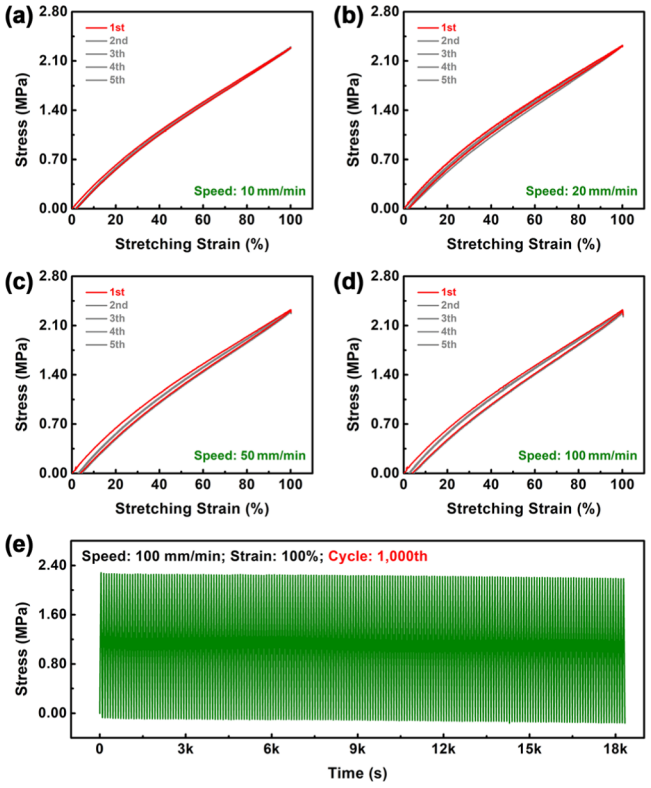

Figure 4. Sequential cyclic tensile curves of BS-PU-3 at 100% deformation in (a) 10; (b) 20; (c) 50; (d) 100 mm/min; (e) fatigue resistance test of BS-PU-3 by sequential cyclic tensile test (1000 times).

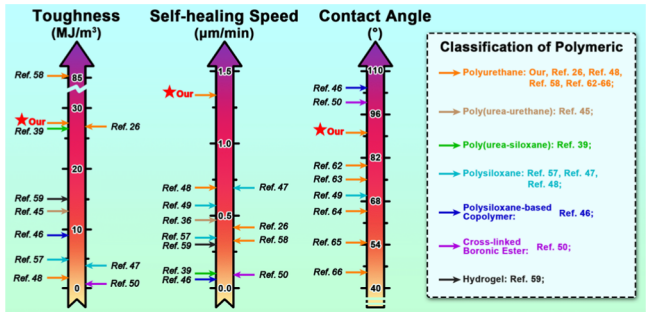

Figure 5. Comparison on toughness (the toughness values recorded in each reference were used directly; because the size and shape of the testing samples are different, such comparison may not be very precise), room-temperature self-healing speed (the self-healing speeds in this comparison were calculated from [notch size]/[self-healing period], where the [notch size] and [self-healing period] were obtained from each reference; because the notch size, shape, and other characteristics of the interfaces varied one by one, such comparison may not be very precise), and hydrophobicity (CWA) among our works and the related references.

curve). A 1 mm notch was cut on a standard dumbbell specimen (ASTM D412), which had a width of 2 mm (Supporting Information, Figure S5), and then the specimen was subjected to a tensile test. All the BS-PU specimens exhibited good tear resistance behavior (Supporting Information, Table S3), of which BS-PU-3 was the best one. The notched BS-PU-3 sample could bear the tensile strain up to 324%, and its fracture toughness was 7.1 MJ/m^3. In contrary, for homopolymers like PDMS, the tear resistance was relatively poor (Supporting Information, Figure S6). This was because the phase structure and the dispersion of stress were homogeneous in these homopolymers, and the dissipation of energy and retardance of notches became difficult. Consequently, the notch would progress easily until the sample breaks.[51] For BS-PU-3, the notch on the dumbbell specimen was blunted and did not extend further during the elongation process, demonstrating its exceptional toughness and tear resistance (Figure 1b). As explained above, the hard domains in PUs acted as the nodes and prevented the notch from expanding. At the notch front, the soft phase sheared greatly and spread large stress on the hard domains. When a hard domain was ruptured, all the elastic energy stored in the highly stretched soft phase would be released.[52−54] Consequently, the microphase-separated morphology could effectively resist tearing in PUs.[39,42] Through DMA, we qualitatively demonstrated the microphase separation in BS-PU-3 (Supporting Information, Figure S7). Subsequently, we used infrared spectroscopy to quantify the degree of phase separation in BS-PU-3, as presented in Figure S8. The characteristic chemical stretching region of the carbonyl group (1650−1810 cm^{-1}) was curve-fitted and resolved into two spectral components by PeakFit software (Figure 1c). The red filled curve (~1700 cm^{-1}) was assigned to the H-bonded carbonyl groups in the hard phase and the blue filled one (~1745 cm^{-1}) corresponded to the free carbonyl groups in the soft matrix. The degree of microphase separation (DPS) was calculated by the following equation[7,8,55,56]

$$\mathrm{DPS} = A_{1700}/(A_{1700} + A_{1745}) \times 100\% \quad (1)$$

where A_{1700} and A_{1745} are the peak areas at 1700 and 1745 cm^{-1}, respectively. A 66.5% of DPS illustrated a good microphase separation in BS-PU-3, which also implied a well-constructed physical network structure. As a result, the higher degree of microphase separation significantly improved the tear resistance and toughness of PUs (Figure S9). In addition, a puncture test of BS-PU-3 was carried out with a pen to simulate the accidental damage that may occur in daily life (Figure 1d). It was seen that BS-PU-3 was effective against puncture without damage. Also, excellent elasticity and toughness could restore it to its original state after puncture (Figure 1d, inset). The above tests clearly proved that the microphase-separated BS-PU-3 could still be fully functional even with accidental notches, which was inevitable during daily use. Strains up to 50−100% (joint motion deformation ability), which are required for the normal operation of the e-skin,[39] should not be a challenge for this material.

However, more damages, including notch, cut, scratch, tear, or even breakage and so forth, could happen to the e-skin. Considering these possibilities, the self-healing ability at ambient temperature becomes very important for the durable use of e-skin. Here, the self-healing ability of the four PUs was tested by an optical microscope equipped with a hot stage. The middle portion of a 0.4 mm thick PU film was cut off, followed by the observation of its self-healing process by the optical microscope (Supporting Information, Figure S10). Taking BS-PU-3 as an example, Figure 2a presents its self-healing process at room temperature. At first, the notch was obvious as a dark line under the microscope. As time went by, the notch faded and became almost invisible after 300 min. The self-healing completed in 360 min. We summarized the self-healing efficiencies of the four PUs at various temperatures (Figure 2b, Supporting Information Figure S11). Obviously, the self-

https://dx.doi.org/10.1021/acsami.0c00443
ACS Appl. Mater. Interfaces 2020, 12, 11072−11083

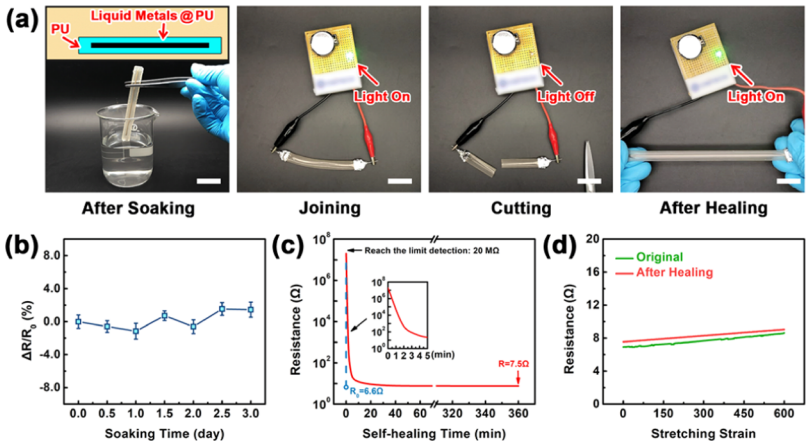

Figure 6. (a) Schematic illustration and optical images of the tough, hydrophobic, and self-healable BS-PU-3 wire equipped with an LED lamp: soaking test, power-on test, self-healing test, and stretching test. Scale bars are all 2 cm; (b) resistance changes of the elastic conductive wire with soaking time; (c) self-healing of the elastic conductive wire resistance after cutting; (d) resistance changes of the elastic conductive wire before cutting and after healing while stretching.

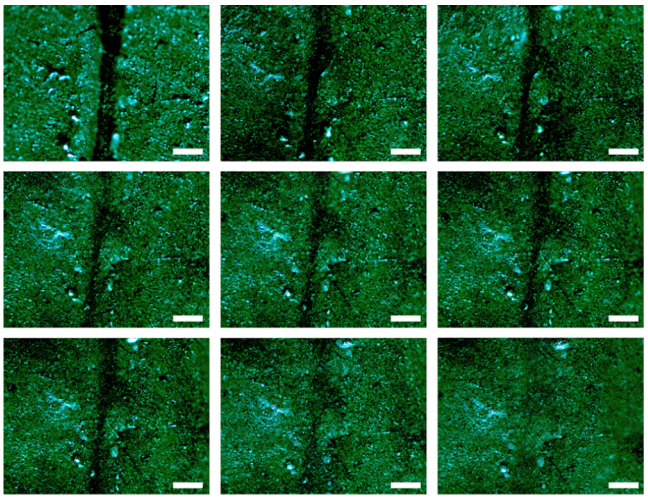

Figure 7. Optical microscopy images of the scratched conductive layer (BS-PU-3/GaInSn) in the self-healing process at 25 °C; 1 h apart for each picture, scale bar: 300 μm.

healing time was related to the notch size. In order to better describe the self-healing ability, we use the self-healing speed to characterize it, that is

$$[\text{Self-healing speed}] = [\text{notch size}]/[\text{self-healing period}]$$

The notch size was the thickness (0.4 mm) of the film. The self-healing speed could be obtained by recording the time when the notch was fully recovered. According to the experimental results, BS-PU-1 and BS-PU-2 did not exhibit self-healing ability at room temperature (25 °C). Nevertheless, they could be self-healed slowly at 50 and 60 °C, respectively. On the other hand, BS-PU-3 and BS-PU-4 were capable of self-healing at room temperature, and the self-healing speed was gradually enhanced as the temperature increased.

Intuitively, the self-healing speed increased with the increasing contents of the dynamic disulfide bonds.[25,26] However, the results in this work were contradictory to such a conjecture. Even with the relatively low dynamic disulfide bond contents of 4.7 mol % and 3.9 mol % of BS-PU-3 and BS-PU-4, respectively, their self-healing speeds were much faster than those of BS-PU-1 and BS-PU-2 (BS-PU-1: 8.5 mol %, BS-PU-2: 5.9 mol %). In this study, the self-healing capability of BS-PUs was not only decided by the content of the dynamic disulfide bond but also closely related to the segmental mobility. With the high hard segment contents and deep microphase separation in BS-PU-1 and BS-PU-2, the physical cross-linking densities were too high and the mobility of soft segments linking the hard domains was seriously depressed. As a result, the process of disulfide metathesis became difficult and the self-healing at room temperature was trivial. Heating above their glass-transition temperature could unfreeze the hard segments and release their self-healing ability.[25] The effects between the dynamic disulfide bond content and segmental mobility on the self-healing property were coupled and interacted with each other. When the content of dynamic disulfide bond was very low, despite the high mobility in the soft domain, the low density of the self-healing point was unable to repair the material with an appreciable speed. When the content of the dynamic disulfide bond was very high, regardless of the high density of the self-healing point, the segmental mobility was too low to allow disulfide metathesis. As a result, we saw fast self-healing speed in BS-PU-3 and BS-PU-4, for their proper content of hard segments and moderate segmental mobility.

The self-healing speeds of BS-PU-3 and BS-PU-4 could be as high as 1.11 and 1.33 μm/min at room temperature, respectively, which were overwhelming among the self-healing materials.[26,39,45−50,57−59] The advantage of the high self-healing speed is obvious that it can repair the damage without taking down the e-skin and keep it working all the time. Such an advance relied on the novel molecular design and was realized by one-pot polymerization. Unlike previously reported PUs with dynamic disulfide bonds,[25,26,45] we adjusted the length and number density of the hard segment along the main chain by one-pot synthesis. Compared to the two-pot synthesized BS-PU-3-2pot, the one-pot synthesized BS-PU-3 had more short-length hard segments connecting the soft segments. In other words, the one-pot synthesis method could induce higher self-healing points because every hard segment concluding dynamic disulfide bonds was a self-healing point. As shown in Figure S12A, the notch in BS-PU-3-2pot experienced slow self-healing at room temperature in 12 h, but the self-healing seemed to stop and kept in incompletion

https://dx.doi.org/10.1021/acsami.0c00443
ACS Appl. Mater. Interfaces 2020, 12, 11072−11083

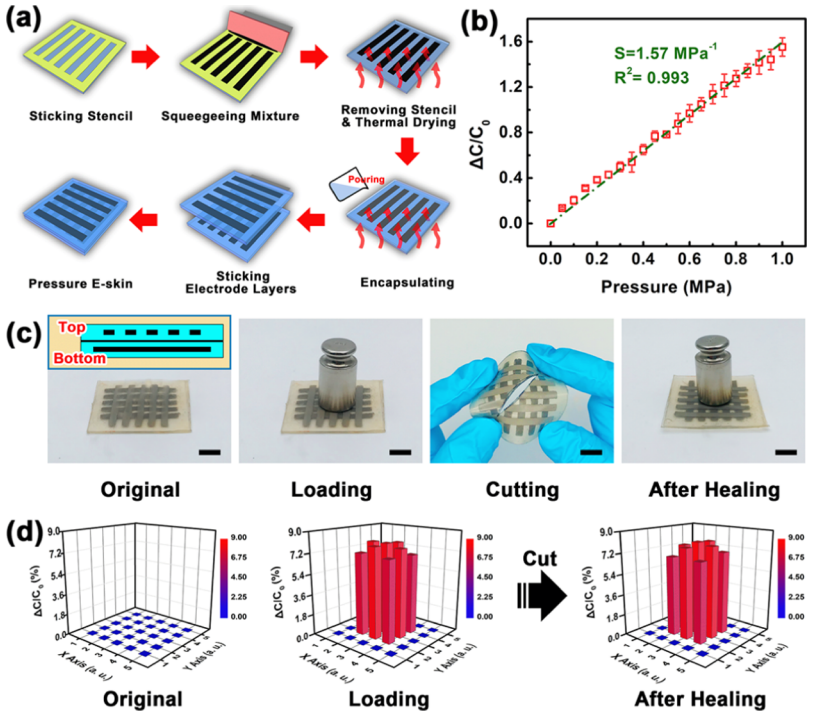

Figure 8. (a) Schematic of the preparation process of the capacitive pressure-sensing e-skin based on BS-PU-3; (b) capacitance changes of each pixel of pressure-sensing e-skin while pressing; (c) schematic illustration and optical images of a 5 × 5 pressure-sensing array detecting a 50 g weight before and after self-healing. Scale bars are all 2 cm; (d) map of the pressure distribution based on the change in capacitance by a 50 g weight before and after self-healing.

after 12 h. By measuring the mechanical properties after self-healing, it was found that the mechanical properties were only recovered to 53% even after 24 h (Supporting Information, Figure S12B). The balance between chain dynamics and the content of the self-healing point was crucial in determining the self-healing behaviors of PUs. In this work, apparently, BS-PU-4 had the best self-healing ability, but BS-PU-3 presented the most balanced properties.

Interestingly, when the experimental temperature reached 60 °C, the self-healing speed of BS-PU-3 even exceeded that of BS-PU-4. This was because the dynamic disulfide bonds were freed from the hard domain at that temperature and BS-PU-3 owned a higher content of dynamic disulfide bonds than that of BS-PU-4. In addition to the superior self-healing speed, the healing effectiveness of BS-PU-3 was evaluated. Two rectangular BS-PU-3 films with about 1 mm thickness, dyed separately by purple and green inks, were cut in half and respliced at 25 °C (Figure 2c). After self-healing, the two rectangular films were firmly bonded together and could withstand a weight of 560 g without any tearing. Again, BS-PU-3 was used to semiquantitatively investigate the self-healing effectiveness. Tensile tests were performed as follows: the standard specimen was cut off in the middle portion, similar to the previous notch repairing test (Supporting Information, Figure S10) and then let to heal by itself to restore the mechanical properties. As shown in Figure 2d, the tensile strength, elongation at break, and toughness increased over time and reached 93% of the original values after 6 h of self-healing at 25 °C. As expected, at the elevated self-healing temperatures (40−60 °C), the mechanical properties recovered after 2 h were further improved to 97%, which was in accordance with the results of the notch repairing test (Figure 2b). The above experiments further demonstrated the superior self-healing speed and ability of BS-PU-3 at a moderate temperature.

As e-skin, longtime use under water or in high relative humidity environment could be imaged. Unfortunately, most PUs could absorb a considerable amount of water. This was because the hydrophilic polyether was usually used as the soft segment and the urethane bond in the hard segment was hydrophilic, too. These two components endowed the PUs with a high water uptake capacity.[60] The PU would deform after water uptake, and the high water content could pose a potential threat to the electrical signals of the electronic device. In this work, the hydrophobic polybutadiene was used as the soft segment in BS-PUs. As minority hydrophilic hard segments and domains were embedded in the polybutadiene matrix, BS-PUs showed an excellent waterproof property. BS-PU-3 and a commercialized sample 1180A (BASF), a typical and frequently used product, were used as examples to evaluate and compare parallelly the waterproof property. The contact water angles (CWA) of the original, 1 day-soaked, and 3 day-soaked BS-PU-3 and 1180A (Figure 3a) were measured. During the soaking experiment, CWA of BS-PU-3 changed little, demonstrating that it was hydrophobic and could hardly absorb water. On the contrary, CWA of 1180A gradually decreased over time, indicating that it became more and more hydrophilic by continuous water absorption. Then, we compared the shape deformation of standard dumbbell specimens after water uptake (Figure 3b). The shape and appearance of the BS-PU-3 specimen did not change at all after soaking in water for 3 days, which could be regarded as an intuitional evidence of good waterproof property. On the other hand, after soaking in water for only 1 day, the color of 1180A changed from transparent to white. After soaking for 3 days, the whitening became more prominent and the sample lost its

https://dx.doi.org/10.1021/acsami.0c00443
ACS Appl. Mater. Interfaces 2020, 12, 11072−11083

original shape and crinkled severely. Clearly, the water absorption could prevent the commercial PU from being used for a long term. Qualitatively, the weights of BS-PU-3 and commercial PU after 3 days of soaking increased by 0.1 and 4.6 wt %, respectively. The hydrophobicity and low water uptake ensured the functionality and durability of BS-PU-3 under water and in a relatively high humidity environment. Furthermore, the mechanical properties and self-healing ability of BS-PU-3 after 3 days of soaking were evaluated (Figure 3c) again. The mechanical properties of the soaked BS-PU-3 sample could still be 95% of the original ones, indicating the negligible effect of water uptake on the mechanical properties. More importantly, the soaked BS-PU-3 specimen still owned fast self-healing capability, as revealed by the tensile behavior of the soaked sample after self-healing (mechanical property recovery: 92%). As the macroscopic behavior was determined by the microscopic structure, we analyzed the phase structure of these two PUs before and after soaking by using SAXS (Figure 3d). With or without soaking, a circular scattering halo could always be seen in the BS-PU-3 sample, which was a typical feature of microphase separation between the soft and hard phases.[38,55,56] The coincidence of one-dimensional integral intensity curves proved the stable microdomain size in BS-PU-3, indicating that water content had no effect on its microstructure (Supporting Information, Figure S13). A weak scattering halo also appeared in the unsoaked 1180A sample, indicating an ambiguous phase structure. After immersing in water for 3 days, no scattering pattern could be discerned anymore, implying the mixing of microdomains, which might be caused by the H-bonding interaction of polytetrahydrofuran and the urethane bonds in 1180A with H_2O molecules.

In order to serve as the matrix of stretchable e-skin, the elastomer is recommended to be tough, with Young's modulus of 5 MPa or less, and its deformability should be preferably above 100%.[1,6,16,17,61] At the same time, the fatigue resistance of the matrix should handle the daily cyclic deformations to make the e-skin durable. Therefore, BS-PU-3 was selected and tested by the sequential cyclic tensile test under 100% deformation. In the cyclic tensile test (Figure 4a), the specimen could get back to its original state without any hysteresis, indicating its excellent antifatigue property. Then, we accelerated the stretching speed, and the curve did not change, proving that the stretching speed did not affect its excellent recoverability (Figure 4b–d). After this, the sequential cyclic tensile test was carried out 1000 times to further evaluate its fatigue resistance (Figure 4e). After 1000 times of cyclic stretching, the tensile strength hardly changed, which proved its excellent fatigue resistance.

Furthermore, based on the room-temperature self-healing ability, excellent tear resistance, and good waterproof behavior, BS-PU-3 deserved to be a good candidate for the elastic matrix of the following e-skin demonstration. Recent lectures have reported that some materials simultaneously had high toughness, room-temperature self-healing, and waterproof properties, or at least two of them.[26,39,45−50,57−59,62−66] Although the sample shape, testing conditions, and so forth were different from one work to another, it was still helpful to roughly compare their toughness, room-temperature self-healing speed, and hydrophobicity (CWA) (Figure 5). It seems that BS-PU-3 prepared in this work had impressive performances in these three aspects. To the best of our knowledge, such a multifunctional PU material with comprehensive and excellent properties has not been developed yet.

For the demonstration of e-skin, we fabricated a stretchable, tough, self-healable, and hydrophobic conductive wire composed of BS-PU-3 as the matrix and GaInSn as the conductive filler. GaInSn is a room-temperature liquid metal (T_m: ∼−15 °C) that is highly conductive and nontoxic, which is considered as an ideal self-healing conductive material based on the microfluidic device structure.[39,67] First, we blended GaInSn with BS-PU-3 (16/1, wt/wt) to prepare a conductive ink. Then, the conductive ink was printed on the surface of the BS-PU-3 film by direct-writing printing technology used in our previous published work.[1] After this, the film was coated by a BS-PU-3 concentrated solution and followed by dry molding (Experimental Section and Figure S14 in the Supporting Information). Finally, an elastic and conductive wire could be obtained based on BS-PU-3 embedding an elastic composite conductor (Figure 6a). Before the test, the wire was soaked in water for 3 days, and no obvious deformation or whitening could be identified. After soaking in water, the resistance change was within 2% (Figure 6b), indicating that the waterproof property of BS-PU-3 protected the inner conductive layer from the water interference. Further, its conductivity was 1.5×10^6 S·m^{-1}, which was high enough to illuminate the light-emitting diode (LED) lamp, showing its stable conductivity even after the critical water uptake test. The prominent self-healing ability of the soaked wire was also examined. The wire was cut into two pieces, and the pieces were stitched together for self-healing at room temperature for 6 h. It was found that the elastic wire could almost fully restore its original mechanical and conductive properties (Supporting Information, Movie S1).

This self-healing process included not only the self-healing of the elastic matrix but also the middle conductive layer. Therefore, we further studied the self-healing process of the conductive layer. First, we detected the change in the resistance of the conductive layer during the self-healing process (Figure 6c). After cutting, the resistance changed from the original 6.6 Ω to infinity, which then gradually recovered to 7.5 Ω after 30 min, much faster than the self-healing speed of BS-PU-3. However, the mechanical properties of this wire took 8 h to recover, and its electrical resistances before and after self-healing changed only slightly (Figure 6d). Lee et al. have reported that the encapsulated liquid metal could restore its conductivity easily and quickly by rupturing the covered thin oxidant layer and flowing to the damaged area.[68,69] Therefore, the electrical properties of the GaInSn liquid metal were restored quickly. On the contrary, the mechanical properties of PU could only be healed by reversible bonds at the interface at a much slower rate. We used an optical microscope to observe the self-healing morphology of the conductive layer (Figure 7). Over time, the conductive layer was self-healed after 8 h, indicating that the self-healing ability of BS-PU-3 was slightly depressed by the GaInSn flow.

The described approach could be easily scalable, for example, we have fabricated a capacitive pressure-sensing e-skin by sandwiching two electrodes, with the BS-PU-3 film acting as a force-sensitive dielectric layer (Figure 8a). In detail, based on the abovementioned elastic wire manufacturing method, a 5 × 5 pressure-sensing array was constructed. The preparation of the upper and lower electrode layers was similar with that of the elastic wire, simply replacing one printed line by five lines of conductive inks. After attaching the two

https://dx.doi.org/10.1021/acsami.0c00443
ACS Appl. Mater. Interfaces 2020, 12, 11072−11083

electrode layers, the intermediate BS-PU-3 encapsulation layer acted as the force-sensitive dielectric layer. During the test, we observed a linear increase of capacitance along with the pressure, which demonstrated that each pixel of our e-skin owns good sensitivity (S = 1.57 MPa^{-1}) and linearity (R^2 = 0.993) to the stimulating pressure in the range of 0−1 MPa (Figure 8b). Furthermore, the fabricated e-skin recognized the pressure distribution successfully when loading a 50 g weight (Figure 8c,d). As expected, the e-skin exhibited appreciable toughness and self-healing ability at room temperature. Even after slicing through the middle portion, the notch would not extend because of the strong toughness of the matrix. The fully functional e-skin was obtained again after self-healing at room temperature for 6 h, recognizing the pressure distribution of a 50 g weight successfully with only a little difference when compared to the original one. As a proof-of-concept, we demonstrated the application of an elastic, tough, hydrophobic, and self-healing electric device based on BS-PU-3.

4. CONCLUSIONS

In summary, we designed and synthesized a PU (BS-PU-3) with excellent and well-balanced properties such as elasticity, toughness, self-healing, and waterproof for application as e-skin. The toughness of BS-PU-3 could be as high as 27.5 MJ/m^3 and resisted tearing effectively. Even with a 1 mm notch (half of the total width) on a standard dumbbell specimen, it could still bear the tensile strain up to 324%. Its self-healing speed at room temperature could reach 1.11 μm/min and the tensile strength of the healed sample could reach 9.4 MPa (original: 9.8 MPa). Young's modulus of this elastomer was 5 MPa, which satisfied the recommended 5 MPa or less for the e-skin matrix, and its elongation was much higher than the required maximum deformability of 100%. No matter it is pure BS-PU-3 or BS-PU-3-based stretchable electronics, the water soaking test did not change their microscopic structure and macroscopic properties, proving the excellent waterproof behavior. These advantages ensure that BS-PU-3 could serve in severe conditions and maintain the functionality of the e-skin. The keys of obtaining well-performed BS-PU-3 are the one-pot synthesis method and the molecular design. The one-pot synthesis method is efficient in obtaining a heterogeneous length distribution of the hard segment and a higher density of self-healing points, which subsequently improve the room-temperature self-healing speed and toughness. In addition, adopting the hydrophobic polybutadiene as the soft segment is successful in obtaining excellent waterproof e-skin. As the synthesis method is feasible to scale-up and the hydrophobic polybutadiene is a commercially available commodity, we suggest that the strategy and material in this work can find wide applications in e-skin and other areas.

■ ASSOCIATED CONTENT

Supporting Information

The Supporting Information is available free of charge at https://pubs.acs.org/doi/10.1021/acsami.0c00443.

One-pot and two-pot polycondensation reactions, ^{1}H-NMR spectra, and 13C-NMR spectra of BS-PUs; contents and components used in the synthesis of BS-PUs; mechanical properties of BS-PU samples and notched BS-PU samples; DMA curves and FTIR spectrum of BS-PUs; self-healing test; optical microscopy images and 1D-SAXS intensity profile of BS-PU-3; and the schematic of the preparation procedures of the elastic conductive wire based on BSPU-3 (PDF)

Restoration of the original mechanical and conductive properties by the elastic wire (MP4)

■ AUTHOR INFORMATION

Corresponding Authors

Jie Shang − *CAS Key Laboratory of Magnetic Materials and Devices, Zhejiang Province Key Laboratory of Magnetic Materials and Application Technolog, Ningbo Institute of Materials Technology and Engineering, Chinese Academy of Sciences, Ningbo 315201, People's Republic of China*; Email: shangjie@nimte.ac.cn

Ruoyu Zhang − *Key Laboratory of Bio-based Polymeric Materials Technology and Application of Zhejiang Province, Ningbo Institute of Materials Technology and Engineering, Chinese Academy of Sciences, Ningbo 315201, People's Republic of China*; orcid.org/0000-0002-3502-8738; Email: zhangruoy@nimte.ac.cn

Authors

Wu Bin Ying − *Key Laboratory of Bio-based Polymeric Materials Technology and Application of Zhejiang Province, Ningbo Institute of Materials Technology and Engineering, Chinese Academy of Sciences, Ningbo 315201, People's Republic of China*; orcid.org/0000-0002-8768-7428

Zhe Yu − *CAS Key Laboratory of Magnetic Materials and Devices, Zhejiang Province Key Laboratory of Magnetic Materials and Application Technolog, Ningbo Institute of Materials Technology and Engineering, Chinese Academy of Sciences, Ningbo 315201, People's Republic of China; College of Materials Science and Opto-Electronic Technology, University of Chinese Academy of Sciences, Beijing 100049, P. R. China*

Do Hwan Kim − *Department of Chemical Engineering, Hanyang University, Seoul 04763, South Korea*; orcid.org/0000-0003-3003-8125

Kyung Jin Lee − *Department of Applied Chemical Engineering, College of Engineering, Chungnam National University, Daejeon 305-764, South Korea*; orcid.org/0000-0002-6709-3235

Han Hu − *Key Laboratory of Bio-based Polymeric Materials Technology and Application of Zhejiang Province, Ningbo Institute of Materials Technology and Engineering, Chinese Academy of Sciences, Ningbo 315201, People's Republic of China*

Yiwei Liu − *CAS Key Laboratory of Magnetic Materials and Devices, Zhejiang Province Key Laboratory of Magnetic Materials and Application Technolog, Ningbo Institute of Materials Technology and Engineering, Chinese Academy of Sciences, Ningbo 315201, People's Republic of China*; orcid.org/0000-0001-9355-5168

Zhengyang Kong − *Key Laboratory of Bio-based Polymeric Materials Technology and Application of Zhejiang Province, Ningbo Institute of Materials Technology and Engineering, Chinese Academy of Sciences, Ningbo 315201, People's Republic of China*

Kai Wang − *Key Laboratory of Bio-based Polymeric Materials Technology and Application of Zhejiang Province, Ningbo Institute of Materials Technology and Engineering, Chinese Academy of Sciences, Ningbo 315201, People's Republic of China*

Jin Zhu − *Key Laboratory of Bio-based Polymeric Materials Technology and Application of Zhejiang Province, Ningbo Institute of Materials Technology and Engineering, Chinese*

https://dx.doi.org/10.1021/acsami.0c00443
ACS Appl. Mater. Interfaces 2020, 12, 11072−11083

Academy of Sciences, Ningbo 315201, People's Republic of China

Run-Wei Li − *CAS Key Laboratory of Magnetic Materials and Devices, Zhejiang Province Key Laboratory of Magnetic Materials and Application Technolog, Ningbo Institute of Materials Technology and Engineering, Chinese Academy of Sciences, Ningbo 315201, People's Republic of China;* orcid.org/0000-0003-3879-9834

Complete contact information is available at: https://pubs.acs.org/10.1021/acsami.0c00443

Author Contributions

#W.B.Y. and Z.Y. contributed equally.

Notes

The authors declare no competing financial interest.

■ ACKNOWLEDGMENTS

This work was supported by National Natural Science Foundation of China (grant no. 51773218), Natural Science Foundation of Zhejiang Province (grant no. LQ19E030005), Ningbo Natural Science Foundation (grant no. 2018A610109), China Postdoctoral Science Foundation (grant no. 2018M632511), Youth Innovation Promotion Association of CAS (2018338), National Natural Foundation of China (61774161), CAS President's International Fellowship Initiative (PIFI) (2019PE0019), Public Welfare Technical Applied Research Project of Zhejiang Province (2017C31100), and Ningbo Scientific and Technological Innovation 2025 Major Project (2018B10057). The authors thank Shanghai Synchrotron Radiation Facility (SSRF) for supporting the SAXS and WAXS tests.

■ REFERENCES

(1) Yu, Z.; Shang, J.; Niu, X.; Liu, Y.; Liu, G.; Dhanapal, P.; Zheng, Y.; Yang, H.; Wu, Y.; Zhou, Y.; Wang, Y.; Tang, D.; Li, R.-W. A Composite Elastic Conductor with High Dynamic Stability Based on 3D-Calabash Bunch Conductive Network Structure for Wearable Devices. *Adv. Electron. Mater.* **2018**, *4*, 1800137.

(2) Tee, B. C. K.; Chortos, A.; Berndt, A.; Nguyen, A. K.; Tom, A.; McGuire, A.; Lin, Z. C.; Tien, K.; Bae, W.-G.; Wang, H.; Mei, P.; Chou, H.-H.; Cui, B.; Deisseroth, K.; Ng, T. N.; Bao, Z. A Skin-Inspired Organic Digital Mechanoreceptor. *Science* **2015**, *350*, 313−316.

(3) Ying, B.; Wu, Q.; Li, J.; Liu, X. An Ambient-stable and Stretchable Ionic Skin with Multimodal Sensation. *Mater. Horiz.* **2020**, *7*, 477−488.

(4) Boutry, C. M.; Negre, M.; Jorda, M.; Vardoulis, O.; Chortos, A.; Khatib, O.; Bao, Z. A Hierarchically Patterned, Bioinspired E-Skin able to Detect The Direction of Applied Pressure for Robotics. *Sci. Robot.* **2018**, *3*, No. eaau6914.

(5) Hammock, M. L.; Chortos, A.; Tee, B. C.-K.; Tok, J. B.-H.; Bao, Z. 25th Anniversary Article: The Evolution of Electronic Skin (E-Skin): A Brief History, Design Considerations, and Recent Progress. *Adv. Mater.* **2013**, *25*, 5997−6038.

(6) Rus, D.; Tolley, M. T. Design, Fabrication and Control of Soft Robots. *Nature* **2015**, *521*, 467−475.

(7) Zhang, L.; Huang, M.; Yu, R.; Huang, J.; Dong, X.; Zhang, R.; Zhu, J. Bio-Based Shape Memory Polyurethanes (Bio-SMPUs) with Short Side Shains in the Soft Segment. *J. Mater. Chem. A* **2014**, *2*, 11490.

(8) Zhang, L.; Shams, S. S.; Wei, Y.; Liu, X.; Ma, S.; Zhang, R.; Zhu, J. Origin of Highly Recoverable Shape Memory Polyurethanes (SMPUs) with Non-Planar Ring Structures: A Single Molecule Force Spectroscopy Investigation. *J. Mater. Chem. A* **2014**, *2*, 20010−20016.

(9) Wang, S.; Oh, J. Y.; Xu, J.; Tran, H.; Bao, Z. Skin-Inspired Electronics: An Emerging Paradigm. *Acc. Chem. Res.* **2018**, *51*, 1033−1045.

(10) Choi, J.; Moon, D. S.; Jang, J. U.; Yin, W. B.; Lee, B.; Lee, K. J. Synthesis of Highly Functionalized Thermoplastic Polyurethanes and Their Potential Applications. *Polymer* **2017**, *116*, 287−294.

(11) Choi, J.; Moon, D. S.; Ryu, S. G.; Lee, B.; Ying, W. B.; Lee, K. J. N-Chloro Hydantoin Functionalized Polyurethane Fibers toward Protective Cloth against Chemical Warfare Agents. *Polymer* **2018**, *138*, 146−155.

(12) Zhang, Z. P.; Rong, M. Z.; Zhang, M. Q. Mechanically Robust, Self-Healable, and Highly Stretchable "Living" Crosslinked Polyurethane Based on a Reversible C-C Bond. *Adv. Funct. Mater.* **2018**, *28*, 1706050.

(13) Hu, W.; Niu, X.; Zhao, R.; Pei, Q. Elastomeric Transparent Capacitive Sensors based on an Interpenetrating Composite of Silver Nanowires and Polyurethane. *Appl. Phys. Lett.* **2013**, *102*, 083303.

(14) Lee, D.; Lee, H.; Jeong, Y.; Ahn, Y.; Nam, G.; Lee, Y. Highly Sensitive, Transparent, and Durable Pressure Sensors Based on Sea-Urchin Shaped Metal Nanoparticles. *Adv. Mater.* **2016**, *28*, 9364−9369.

(15) Zhang, Q.; Niu, S.; Wang, L.; Lopez, J.; Chen, S.; Cai, Y.; Du, R.; Liu, Y.; Lai, J. C.; Liu, L.; Li, C. H.; Yan, X.; Liu, C.; Tok, J. B.; Jia, X.; Bao, Z. An Elastic Autonomous Self-Healing Capacitive Sensor Based on a Dynamic Dual Crosslinked Chemical System. *Adv. Mater.* **2018**, *30*, 1801435.

(16) Wang, C.; Wang, C.; Huang, Z.; Xu, S. Materials and Structures toward Soft Electronics. *Adv. Mater.* **2018**, *30*, 1801368.

(17) Wang, S.; Oh, J. Y.; Xu, J.; Tran, H.; Bao, Z. Skin-Inspired Electronics: An Emerging Paradigm. *Acc. Chem. Res.* **2018**, *51*, 1033−1045.

(18) Li, T.; Li, Y.; Zhang, T. Materials, Structures, and Functions for Flexible and Stretchable Biomimetic Sensors. *Acc. Chem. Res.* **2019**, *52*, 288−296.

(19) Chortos, A.; Liu, J.; Bao, Z. Pursuing Prosthetic Electronic Skin. *Nat. Mater.* **2016**, *15*, 937−950.

(20) Wei, M.; Zhan, M.; Yu, D.; Xie, H.; He, M.; Yang, K.; Wang, Y. Novel Poly (tetramethylene ether) glycol and Poly (ε-caprolactone) based Dynamic Network via Quadruple Hydrogen Bonding with Triple-Shape Effect and Self-healing Capacity. *ACS Appl. Mater. Interfaces* **2015**, *7*, 2585−2596.

(21) Pu, W.; Fu, D.; Wang, Z.; Gan, X.; Lu, X.; Yang, L.; Xia, H. Realizing Crack Diagnosing and Self-Healing by Electricity with a Dynamic Crosslinked Flexible Polyurethane Composite. *Adv. Sci.* **2018**, *5*, 1800101.

(22) Wang, Z.; Xie, C.; Yu, C.; Fei, G.; Wang, Z.; Xia, H. A Facile Strategy for Self-Healing Polyurethanes Containing Multiple Metal-Ligand Bonds. *Macromol. Rapid Commun.* **2018**, *39*, 1700678.

(23) Liu, W.-X.; Yang, Z.; Qiao, Z.; Zhang, L.; Zhao, N.; Luo, S.; Xu, J. Dynamic Multiphase Semi-Crystalline Polymers based on Thermally Reversible Pyrazole-Urea Bonds. *Nat. Commun.* **2019**, *10*, 4753.

(24) Wang, Z.; Gangarapu, S.; Escorihuela, J.; Fei, G.; Zuilhof, H.; Xia, H. Dynamic Covalent Urea Bonds and Their Potential for Development of Self-Healing Polymer Materials. *J. Mater. Chem. A* **2019**, *7*, 15933−15943.

(25) Lai, Y.; Kuang, X.; Zhu, P.; Huang, M.; Dong, X.; Wang, D. Colorless, Transparent, Robust, and Fast Scratch-Self-Healing Elastomers via a Phase-Locked Dynamic Bonds Design. *Adv. Mater.* **2018**, *30*, 1802556.

(26) Kim, S.-M.; Jeon, H.; Shin, S.-H.; Park, S.-A.; Jegal, J.; Hwang, S. Y.; Oh, D. X.; Park, J. Superior Toughness and Fast Self-Healing at Room Temperature Engineered by Transparent Elastomers. *Adv. Mater.* **2018**, *30*, 1705145.

(27) Wang, Z.; Lu, X.; Sun, S.; Yu, C.; Xia, H. Preparation, Characterization and Properties of Intrinsic Self-Healing Elastomers. *J. Mater. Chem. B* **2019**, *7*, 4876−4926.

(28) Amrollahi, M.; Sadeghi, G. M. M. Assessment of Adhesion and Surface Properties of Polyurethane Coatings based on Non-Polar and Hydrophobic Soft Segment. *Prog. Org. Coat.* **2016**, *93*, 23−33.
(29) Bandelli, D.; Helbing, C.; Weber, C.; Seifert, M.; Muljajew, I.; Jandt, K. D.; Schubert, U. S. Maintaining the Hydrophilic−Hydrophobic Balance of Polyesters with Adjustable Crystallinity for Tailor-Made Nanoparticles. *Macromolecules* **2018**, *51*, 5567−5576.
(30) Kakde, D.; Taresco, V.; Bansal, K. K.; Magennis, E. P.; Howdle, S. M.; Mantovani, G.; Irvine, D. J.; Alexander, C. Amphiphilic Block Copolymers from a Renewable ε-Decalactone Monomer: Prediction and Characterization of Micellar Core Effects on Drug Encapsulation and Release. *J. Mater. Chem. B* **2016**, *4*, 7119−7129.
(31) Malkappa, K.; Rao, B. N.; Jana, T. Functionalized Polybutadiene dDiol based Hydrophobic, Water Dispersible Polyurethane Nanocomposites: Role of Organo-Clay Structure. *Polymer* **2016**, *99*, 404−416.
(32) Tsen, W.-C.; Lee, C.-F.; Su, Y.-R.; Gu, J.-H.; Suen, M.-C. Effect of Novel Aliphatic Fluoro-Diol Content on Synthesis and Properties of Waterborne Polyurethanes. *J. Appl. Polym. Sci.* **2019**, *136*, 47356.
(33) Miller, J. A.; Lin, S. B.; Hwang, K. K. S.; Wu, K. S.; Gibson, P. E.; Cooper, S. L. Properties of Polyether-Polyurethane Block Copolymers: Effects of Hard Segment Length Distribution. *Macromolecules* **1985**, *18*, 32−44.
(34) Koyo, H.; Tsuruta, T.; Kataoka, K. Synthesis of Novel Types of Segmented Polyamineurea and Polyamine-Poly(ethylene oxide) Block Copolymer. *Polym. J.* **1993**, *25*, 141−152.
(35) Krol, P. Synthesis Methods, Chemical Structures and Phase Structures of Linear Polyurethanes. Properties and Applications of Linear Polyurethanes in Polyurethane Elastomers, Copolymers and Ionomers. *Prog. Mater. Sci.* **2007**, *52*, 915−1015.
(36) Yilgör, I.; Yilgör, E.; Wilkes, G. L. Critical Parameters in Designing Segmented Polyurethanes and Their Effect on Morphology and Properties: A Comprehensive Review. *Polymer* **2015**, *58*, A1−A36.
(37) Leung, L. M.; Koberstein, J. T. Dsc Annealing Study of Microphase Separation and Multiple Endothermic Behavior in Polyether-Based Polyurethane Block Copolymers. *Macromolecules* **1986**, *19*, 706−713.
(38) Wang, C. B.; Cooper, S. L. Morphology and Properties of Segmented Polyether Polyurethaneureas. *Macromolecules* **1983**, *16*, 775−786.
(39) Kang, J.; Son, D.; Wang, G. N.; Liu, Y.; Lopez, J.; Kim, Y.; Oh, J. Y.; Katsumata, T.; Mun, J.; Lee, Y.; Jin, L.; Tok, J. B.; Bao, Z. Tough and Water-Insensitive Self-Healing Elastomer for Robust Electronic Skin. *Adv. Mater.* **2018**, *30*, 1706846.
(40) Hsieh, H. L.; Quirk, R. P. *Anionic Polymerization: Principles and Practical Applications*; Marcel Dekker: New York, 1996; Vol. *18*, pp 476−479.
(41) Peng, Y.; Zhao, L.; Yang, C.; Yang, Y.; Song, C.; Wu, Q.; Huang, G.; Wu, J. Super Tough and Strong Self-Healing Elastomers based on Polyampholytes. *J. Mater. Chem. A* **2018**, *6*, 19066−19074.
(42) Kong, Z.; Tian, Q.; Zhang, R.; Yin, J.; Shi, L.; Ying, W. B.; Hu, H.; Yao, C.; Wang, K.; Zhu, J. Reexamination Of The Microphase Separation in MDI and PTMG based Polyurethane: Fast and Continuous Association/Dissociation Processes of Hydrogen Bonding. *Polymer* **2019**, *185*, 121943.
(43) Malkappa, K.; Rao, B. N.; Jana, T. Functionalized Polybutadiene Diol based Hydrophobic, Water Dispersible Polyurethane Nanocomposites: Role of Organo-Clay Structure. *Polymer* **2016**, *99*, 404−416.
(44) Cao, Z.; Zhou, Q.; Jie, S.; Li, B.-G. High Cis-1, 4 Hydroxyl-Terminated Polybutadiene-based Polyurethanes with Extremely Low Glass Transition Temperature and Excellent Mechanical Properties. *Ind. Eng. Chem. Res.* **2016**, *55*, 1582−1589.
(45) Rekondo, A.; Martin, R.; de Luzuriaga, A. R.; Cabañero, G.; Grande, H. J.; Odriozola, I. Catalyst-Free Room-Temperature Self-Healing Elastomers based on Aromatic Disulfide Metathesis. *Mater. Horiz.* **2014**, *1*, 237−240.
(46) Jin, B.; Liu, M.; Zhang, Q.; Zhan, X.; Chen, F. Silicone Oil Swelling Slippery Surfaces Based on Mussel-Inspired Magnetic Nanoparticles with Multiple Self-Healing Mechanisms. *Langmuir* **2017**, *33*, 10340−10350.
(47) Mei, J.-F.; Jia, X.-Y.; Lai, J.-C.; Sun, Y.; Li, C.-H.; Wu, J.-H.; Cao, Y.; You, X.-Z.; Bao, Z. A Highly Stretchable and Autonomous Self-Healing Polymer Based on Combination of Pt...Pt and pi-pi Interactions. *Macromol. Rapid Commun.* **2016**, *37*, 1667−1675.
(48) Amamoto, Y.; Otsuka, H.; Takahara, A.; Matyjaszewski, K. Self-Healing of Covalently Cross-Linked Polymers by Reshuffling Thiuram Disulfide Moieties in Air under Visible Light. *Adv. Mater.* **2012**, *24*, 3975−3980.
(49) Kathan, M.; Kovaříček, P.; Jurissek, C.; Senf, A.; Dallmann, A.; Thünemann, A. F.; Hecht, S. Control of Imine Exchange Kinetics with Photoswitches to Modulate Self-Healing in Polysiloxane Networks by Light Illumination. *Angew. Chem., Int. Ed.* **2016**, *55*, 13882−13886.
(50) Cash, J. J.; Kubo, T.; Bapat, A. P.; Sumerlin, B. S. Room-Temperature Self-Healing Polymers Based on Dynamic-Covalent Boronic Esters. *Macromolecules* **2015**, *48*, 2098−2106.
(51) Keller, M. W.; White, S. R.; Sottos, N. R. A Self-Healing Poly(Dimethyl Siloxane) Elastomer. *Adv. Funct. Mater.* **2007**, *17*, 2399−2404.
(52) Kazem, N.; Bartlett, M. D.; Majidi, C. Extreme Toughening of Soft Materials with Liquid Metal. *Adv. Mater.* **2018**, *30*, 1706594.
(53) Wang, Z.; Xiang, C.; Yao, X.; Le Floch, P.; Mendez, J.; Suo, Z. Stretchable Materials of High Toughness and Low Hysteresis. *Proc. Natl. Acad. Sci. U.S.A.* **2019**, *116*, 5967−5972.
(54) Xiang, C.; Wang, Z.; Yang, C.; Yao, X.; Wang, Y.; Suo, Z. Stretchable and Fatigue-Resistant Materials. *Mater. Today* **2019**, DOI: 10.1016/j.mattod.2019.08.009.
(55) Guo, Y.; Zhang, R.; Xiao, Q.; Guo, H.; Wang, Z.; Li, X.; Chen, J.; Zhu, J. Asynchronous Fracture of Hierarchical Microstructures in Hard Domain of Thermoplastic Polyurethane Elastomer: Effect of Chain Extender. *Polymer* **2018**, *138*, 242−254.
(56) Xu, W.; Zhang, R.; Liu, W.; Zhu, J.; Dong, X.; Guo, H.; Hu, G.-H. A Multiscale Investigation on the Mechanism of Shape Recovery for IPDI to PPDI Hard Segment Substitution in Polyurethane. *Macromolecules* **2016**, *49*, 5931−5944.
(57) Li, C.-H.; Wang, C.; Keplinger, C.; Zuo, J.-L.; Jin, L.; Sun, Y.; Zheng, P.; Cao, Y.; Lissel, F.; Linder, C.; You, X.-Z.; Bao, Z. A Highly Stretchable Autonomous Self-Healing Elastomer. *Nat. Chem.* **2016**, *8*, 618−624.
(58) Zhang, L.; Liu, Z.; Wu, X.; Guan, Q.; Chen, S.; Sun, L.; Guo, Y.; Wang, S.; Song, J.; Jeffries, E. M.; He, C.; Qing, F. L.; Bao, X.; You, Z. A Highly Efficient Self-Healing Elastomer with Unprecedented Mechanical Properties. *Adv. Mater.* **2019**, *31*, 1901402.
(59) Wang, P.; Deng, G.; Zhou, L.; Li, Z.; Chen, Y. Ultrastretchable, Self-Healable Hydrogels Based on Dynamic Covalent Bonding and Triblock Copolymer Micellization. *ACS Macro Lett.* **2017**, *6*, 881−886.
(60) Kang, K. S.; Jee, C.; Bae, J.-H.; Jung, H. J.; Kim, B. J.; Huh, P. Effect of Soft/Hard Segments in Poly (Tetramethylene Glycol)-Polyurethane for Water Barrier Film. *Prog. Org. Coat.* **2018**, *123*, 238−241.
(61) Yao, S.; Zhu, Y. Nanomaterial-Enabled Stretchable Conductors: Strategies, Materials and Devices. *Adv. Mater.* **2015**, *27*, 1480−1511.
(62) Acik, G.; Kamaci, M.; Altinkok, C.; Karabulut, H. R. F.; Tasdelen, M. A. Synthesis and Properties of Soybean Oil-based Biodegradable Polyurethane Films. *Prog. Org. Coat.* **2018**, *123*, 261−266.
(63) Liu, L.; Lu, J.; Zhang, Y.; Liang, H.; Liang, D.; Jiang, J.; Lu, Q.; Quirino, R. L.; Zhang, C. Thermosetting Polyurethanes Prepared with the Aid of a Fully Bio-based Emulsifier with High Bio-Content, High Solid Content, and Superior Mechanical Properties. *Green Chem.* **2019**, *21*, 526−537.
(64) Tsou, C.-H.; Lee, H.-T.; Hung, W.-S.; Wang, C.-C.; Shu, C.-C.; Suen, M.-C.; De Guzman, M. Synthesis and Properties of

Antibacterial Polyurethane with Novel Bis(3-Pyridinemethanol) Silver Chain Extender. *Polymer* **2016**, *85*, 96−105.
(65) Chen, S.; Mo, F.; Yang, Y.; Stadler, F. J.; Chen, S.; Yang, H.; Ge, Z. Development of Zwitterionic Polyurethanes with Multi-Shape Memory Effects and Self-Healing Properties. *J. Mater. Chem. A* **2015**, *3*, 2924−2933.
(66) Yuan, H.; Qian, B.; Zhang, W.; Lan, M. Protein Adsorption Resistance of PVP-Modified Polyurethane Film Prepared by Surface-Initiated Atom Transfer Radical Polymerization. *Appl. Surf. Sci.* **2016**, *363*, 483−489.
(67) Dickey, M. D. Stretchable and Soft Electronics using Liquid Metals. *Adv. Mater.* **2017**, *29*, 1606425.
(68) Wang, J.; Cai, G.; Li, S.; Gao, D.; Xiong, J.; Lee, P. S. Printable Superelastic Conductors with Extreme Stretchability and Robust Cycling Endurance Enabled by Liquid-Metal Particles. *Adv. Mater.* **2018**, *30*, 1706157.
(69) Park, S.; Thangavel, G.; Parida, K.; Li, S.; Lee, P. S. A Stretchable and Self-Healing Energy Storage Device Based on Mechanically and Electrically Restorative Liquid-Metal Particles and Carboxylated Polyurethane Composites. *Adv. Mater.* **2019**, *31*, 1805536.

https://dx.doi.org/10.1021/acsami.0c00443
ACS Appl. Mater. Interfaces 2020, 12, 11072−11083